

# Thermophysical Properties of Ethylene Glycol Dispersed with $\text{Al}_2\text{O}_3$ Nanoparticles for Solar Thermal Applications

**Ms. Ardhani Satya Bhanu Prasanna**

<sup>1</sup>\*Associate Professor, Baba Institute of Technology and Sciences Vishakhapatnam, India

**Dr. K Ramji**

<sup>2</sup>Professor, Department of Mechanical Engineering, AU College of Engineering, India

**\*Corresponding Author:** Ms. Ardhani Satya Bhanu Prasanna

E-mail: satyabhanuprasanna@gmail.com

## ABSTRACT

This study focuses on investigating the effects of adding Aluminium oxide ( $\text{Al}_2\text{O}_3$ ) nanoparticles in ethylene glycol with emphasis on thermal conductivity and heat transfer enhancement. Alumina ( $\text{Al}_2\text{O}_3$ ) nanoparticles after surface modification with a surfactant cetrimonium bromide (CTAB) were dispersed at concentrations of 1, 0.5, 0.25, and 0.125 mass percentages in ethylene glycol. The thermal conductivity and dynamic viscosity with different concentrations are evaluated, and through these properties, the heat transfer efficacy of nanofluids is evaluated indirectly using a figure of merit called Mouromtseff number (Mo). The stability of suspension dispersed with CTAB is found to be excellent and the nanofluids could remain stable for one month. The addition of  $\text{Al}_2\text{O}_3$  nanoparticles to ethylene glycol leads to a significant improvement in thermal conductivity, ranging from 15% to 25%. The Mouromtseff number (Mo) indicates that in turbulent flow, dilute nanofluids with low concentrations are the most efficient heat transfer medium.

**Keywords:** solar thermal applications; nanofluids; aluminium oxide nanoparticles; zeta potential; dynamic viscosity; thermal conductivity enhancement; correlations

## Nomenclature

$k$  = Thermal conductivity (W/m/ K).

T= Temperature

Roman letters

$\mu$  = Dynamic viscosity (centipoise, cP).

$\rho$  = Density of the fluid ( $\text{kg/m}^3$ )

$f$  = weight fraction of  $\text{Al}_2\text{O}_3$  nanoparticles

Subscripts

$nf$  nanofluid

$b$  Base fluids

$\text{max}$  Maximum temperature

Abbreviations

DM water – demineralized water

EG – Ethylene glycol

## 1 INTRODUCTION

Energy studies have focused on optimizing renewable energy sources. Solar energy is the most popular renewable energy. Solar energy can be used for building heating and cooling, domestic water heating, water desalination, and many industrial applications [2–4]. Several developments have improved solar energy use [5] and storage [6]. Modern advances, especially in solar thermal collector technology, have increased solar energy consumption. A substance absorbs solar radiation in the solar thermal collector's heat exchanger. The thermal energy is transferred to a working fluid like air, water, nanofluid, or oil for many different applications. Evacuated tube solar collector systems are vital in delivering heat to the heat transfer fluid or working fluid. Solar collectors are devices that

have the ability to capture waves and transform solar radiation into either thermal or electrical energy [7]. Ethylene glycol, also referred to as momo ethylene glycol, is a water-soluble compound with the chemical formula  $(\text{CH}_2\text{OH})_2$ . It is commonly employed in the thermal regulation of engineering systems.

Although there have been gradual improvements in the thermal efficiency of these collectors throughout time, it is crucial to continue boosting their efficiency until they reach the highest possible level. The use of nanofluids has significant potential to improve the thermal efficiency of heat-collecting systems. Choi and Eastman [8] found that using nanoparticle dispersions can improve the thermal conductivity properties of base fluids. Several researchers have

endeavored to utilize these nanofluids in various heat transfer systems, and their empirical findings have demonstrated varying degrees of achievement [9–10]. Previous studies [1–30] have demonstrated that nanofluids have enhanced thermal conductivity in comparison to the base fluid.

Extensive study has shown that water-based fluids have a narrow working temperature range because of the freezing and evaporation properties of water. Conversely, the fluids containing ethylene glycol (EG) have a far broader spectrum of temperatures they may function within, ranging from  $-12.9\text{ }^{\circ}\text{C}$  to  $197.3\text{ }^{\circ}\text{C}$ . The extended temperature range provides the possibility Alumina nanoparticles, or aluminum oxide ( $\text{Al}_2\text{O}_3$ ) nanoparticles, provide numerous benefits compared to other nanoparticles when utilized in nanofluids. Alumina nanoparticles exhibit exceptional thermal stability and can endure elevated temperatures without undergoing degradation. These properties make them well-suited for applications that necessitate high temperatures, such as cooling electrical equipment and industrial operations operating at excessive temperatures. Alumina nanoparticles exhibit a comparatively elevated heat conductivity. When the particles are distributed in a fluid, they have the ability to greatly improve the thermal conductivity of the nanofluid. This characteristic is advantageous for enhancing the efficiency of heat transmission in different systems, such as heat exchangers and applications related to thermal management. Alumina nanoparticles generally possess a substantial surface area, which aids in their dispersion into the underlying fluid. Increasing the surface area can augment their contact with the fluid and enhance the overall performance of the nanofluid.

Seedhara and Satapathy (2020) present a concise overview of the production process for  $\text{Al}_2\text{O}_3$  nanofluid and the variables that influence the enhancement of thermal conductivity. Research has shown that  $\text{Al}_2\text{O}_3$  nanofluid exhibits excellent heat conduction properties and is highly appropriate for real-world heat transfer applications. Cho et.al [9] examined the impact of  $\text{Al}_2\text{O}_3$  nanofluid on the thermal characteristics of the circular enclosure, which functions as a medium for heat recovery in the stack. By incorporating a nanofluid with a 0.1 vol%- $\text{Al}_2\text{O}_3$  concentration, the fluid experienced a 3.4% increase in temperature, a 20.6% increase in convective heat transfer coefficient, a 7.15%

increase in heat flux, and a 22.04% increase in Nusselt number. Nanoparticles aggregate, leading to their sedimentation in the liquid, hence diminishing the thermal conductivity of nanofluids. Hence, it is crucial to analyze and evaluate the factors that influence the stability of nanoparticle dispersion. The production of nanofluids typically follows a two-step process, wherein nanoparticles are initially synthesized and subsequently dispersed into the base fluids [20]. The two-step approach is frequently employed for nanofluid synthesis owing to its capacity to effectively control the volume fractions of nanoparticles in the mixture.

Numerous researchers have researched the impact of nanoparticle size and concentration on heat transfer inside tubes. Nevertheless, there has been limited investigation into the improvement of heat transmission in helical heat exchangers using nanofluids, which is the unique aspect of our study. The work involved the fabrication of nanofluids comprising of  $\text{Al}_2\text{O}_3$  nanoparticles with surface modification. Zeta potential assessment was used to examine the stability of these nanofluids over a duration of 30 days. The study also included the measurement and evaluation of the fluid's dynamic viscosity, thermal conductivity, and enhancement of heat transfer. The incorporation of  $\text{Al}_2\text{O}_3$  nanoparticles into ethylene glycol was achieved by using different weight percentages (1, 0.5, 0.25, and 0.125 wt%). This study provides comprehensive correlations for calculating the dynamic viscosity and thermal conductivity. The efficacy of the nanomaterials in enhancing heat transmission is assessed in the experimental configuration by employing a heat exchanger with a coil-shaped design. Analyzed heat transfer statistics were utilized to develop a full correlation for the Nusselt number.

## 2 Methods and Experimentation

### Preparation of nanofluids and assessing its stability

In the current study, ethylene glycol was chosen as base fluids and surface modified  $\text{Al}_2\text{O}_3$  nano particles were disseminated in base fluids at concentrations of 1, 0.5, 0.25, 0.125, and 0.0625 wt% using a probe ultrasonicator. Their details are presented in Table 1. The fluids underwent sonication for a duration of thirty minutes subsequent to the mixing of the  $\text{Al}_2\text{O}_3$ , in order to attain a homogeneous dispersion of the nanomaterials.

TABLE 1: Base fluids description

S.No	Composition
1	Ethylene glycol
2	Ethylene glycol - 1 % $\text{Al}_2\text{O}_3$ nanoparticles
3	Ethylene glycol - 0.5 % $\text{Al}_2\text{O}_3$ nanoparticles
4	Ethylene glycol - 0.25 % $\text{Al}_2\text{O}_3$ nanoparticles
5	Ethylene glycol - 0.125 % $\text{Al}_2\text{O}_3$ nanoparticles

Non-covalent functionalization or dispersants/surfactants are the most frequent ways to stabilize nanofluids and avoid nanoparticle clumping. Reduce base fluid surface tension. Dispersant overuse can impair nanofluid thermal conductivity and chemical stability [20]. Thus, dispersant dosage must be optimized. A hydrophilic polar head group and a hydrophobic tail of long-chain hydrocarbons make up surfactants. Polyvinylpyrrolidone (PVP), SDBS, Gum arabic, SDS, CTAB, DTAB, and Oleic Acid are common

dispersants. CTAB and SDS helped prepare stable nanofluid suspensions in this work.

## 2.1 Characterizations of nanoparticles

The  $\text{Al}_2\text{O}_3$  nanoparticle structure was examined with a transmission electron microscope. A transmission electron microscope can give high-clarity images of nanoparticles. As can be seen in Figure 1, the particles are clearly visible and seem to be circular with an average diameter of nearly 50 nm.

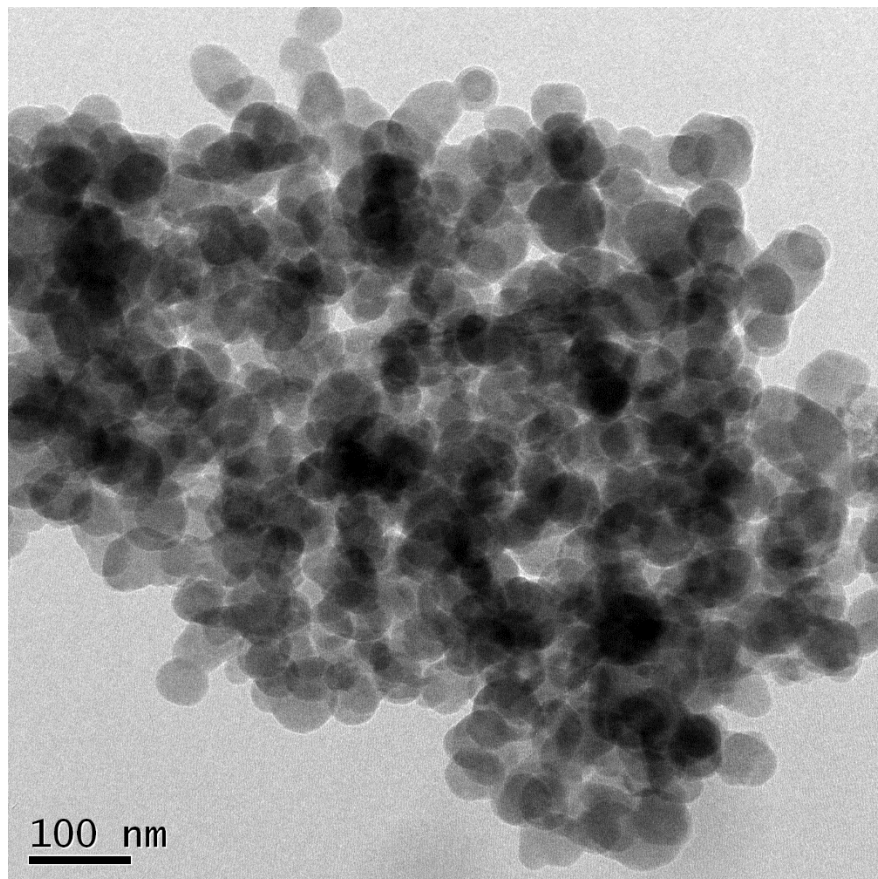
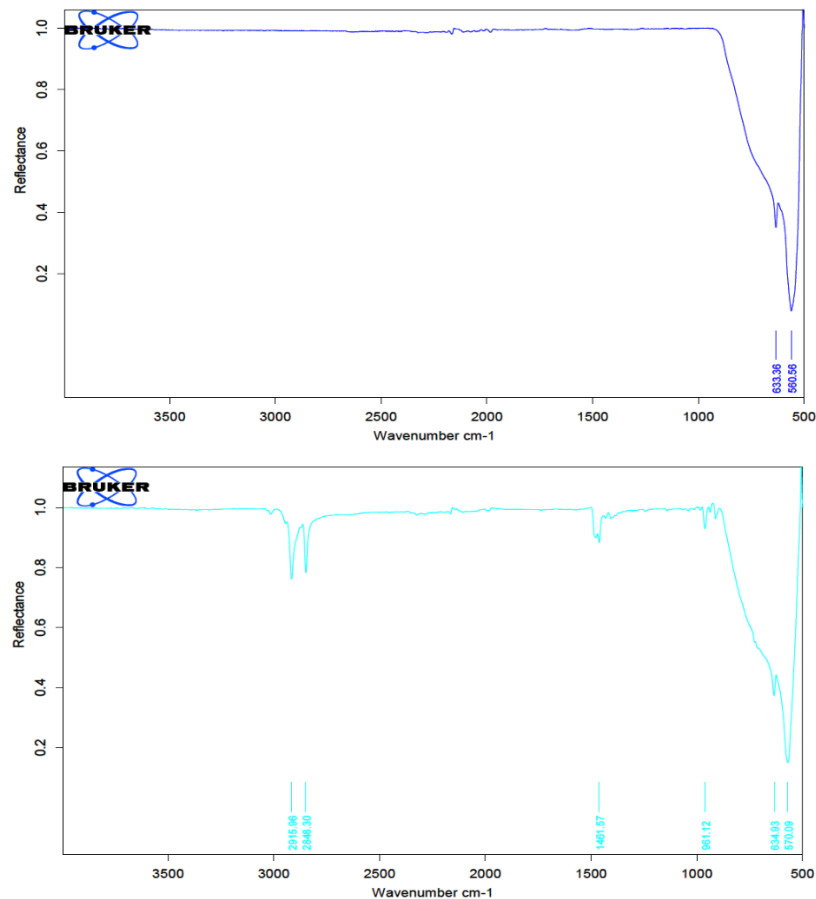


FIG. 1: HRTEM pictograph of  $\text{Al}_2\text{O}_3$  nanoparticles

Fourier transform infrared spectroscopy (FTIR) is used to acquire the absorption or emission infrared spectrum (IR) of a given sample. The Fourier transform infrared spectrometer (FTIR) efficiently collects data with high spectral resolution over a broad range of wavelengths allowing the

measurement of light transmission components through the material. FTIR spectroscopy was employed to characterize the treated  $\text{Al}_2\text{O}_3$  in order to identify the presence of functional groups. In Fig. 2 the IR spectrum of pristine and surface modified  $\text{Al}_2\text{O}_3$  nano particles is presented.



**Fig. 2** Infra-red spectroscopy of a) pristine  $\text{Al}_2\text{O}_3$  and b)  $\text{Al}_2\text{O}_3$  surface-modified with CTAB

The spectra of untreated and treated  $\text{Al}_2\text{O}_3$  is depicted in Fig. 2a. aluminum oxide ( $\text{Al}_2\text{O}_3$ ), has specific vibrational modes that can be identified in the FTIR spectrum. The peaks identifying Al-O stretching vibrations is observed in the range of 600-800  $\text{cm}^{-1}$ . The Al-O bending vibrations can be seen in the range of 400-600  $\text{cm}^{-1}$ . The modified  $\text{Al}_2\text{O}_3$ , as observed in Fig. 2b, has both exhibited alumina spectra as well as the spectra of CTAB. Quaternary ammonium group absorption bands were observed around 2800-3100  $\text{cm}^{-1}$  (stretching vibrations of C-H bonds) and 1400-1500  $\text{cm}^{-1}$  (bending vibrations). Bromide ion ( $\text{Br}^-$ ) absorption band can be seen in the region of 500-600  $\text{cm}^{-1}$ .

The subsequent part will address the preparation of nanofluids and assessment of their stability using zeta potential analysis.

## 2.5 Estimation thermal conductivity and dynamic viscosity

Convection-based heat transport in liquids makes measuring thermal conductivity harder than in solids. The ASTM D7984-compliant C-Therm trident MTPS sensor measures thermal conductivity and effusivity using Modified Transient Plane Source (MTPS) technology. A one-sided, interfacial heat reflectance sensor heats the sample briefly and consistently. Electricity is transmitted to the sensor's coiled heating component, generating some thermal energy. A protective ring around the sensor

coil allows unidirectional heat passage into the sample. The current provided raises the sensor-sample interface temperature, changing the sensor element's voltage drop. Sample thermal properties are determined by sensor voltage change. At the sensor-sample interface, thermal conductivity decreases with temperature increase. When evaluating materials with lower heat conductivity, voltage rises faster. Better heat conductivity materials have a shallower voltage slope. Usually, the measurement pulse lasts 10–20 seconds. Thermal conductivity and effusivity measurements provide a complete heat transfer assessment of the sample material. Its properties make it ideal for testing nanofluid thermal conductivity. The MTPS sensor was utilized because its short measuring duration reduces convection errors.

Technique or procedure: Wells-Brookfield approach. Base and nanofluid absolute viscosities were measured with the Cone & Plate Viscometer. The Cone and Plate Viscometer measures torque at specific rotational speeds. A precisely calibrated beryllium-copper spring connects the drive mechanism to a rotating cone for torque measurement. This apparatus measures sample fluid rotation resistance between the cone and a stationary flat plate. Against the cone's rotation, torque is directly related to fluid shear stress. Torque is shown by a dial or digital display,

depending on type. You can easily convert this data to absolute centipoise units (mPa·s) using pre-calculated range charts.

The specimens indicated in Table 1 were prepared and examined to determine their thermal conductivity and dynamic viscosity at different temperatures. In order to maintain the uniformity and ability to replicate the results, three distinct trials were conducted, wherein each experiment comprised of five duplicate samples conducted at varying temperatures. The testing period for thermal conductivity and viscosity was modified to assess the coherence of the gathered data. The mean of all recorded readings at a specific temperature is documented.

### 3 Results and discussion

#### 3.1 Analysis of Fluid Stability Using Zeta Potential Analysis

The stability of colloidal fluids is evaluated by measuring the zeta potential of the fluid. The zeta potential quantifies the degree of electrostatic repulsion between charged particles. A critical threshold of  $\pm 25$  is indicative of the progressive stabilization of the solution, whereas values surpassing 25 and falling below -25 indicate a high level of stability in the nanofluids. The stability of ethylene glycol-water mixtures combined with surface modified  $\text{Al}_2\text{O}_3$  is evaluated by assessing their zeta potential over a period of 30 days. The stability of all the nanofluids was assessed over a period of one month, and the corresponding outcomes are presented in Table 2 and 3. Figs 3 and 4 depict the zeta potential values of specific coolants. Figure 3 displays the zeta potential of nanofluids containing 1% pure  $\text{Al}_2\text{O}_3$ . It is evident from the graph that the zeta potential exhibits a very low value both on the initial day and after a period of 5 days. Figure 4 illustrates the temporal evolution of

zeta potential in nanofluids over a span of 30 days. The dispersion of surface-modified  $\text{Al}_2\text{O}_3$  nanoparticles exhibited remarkable stability over this period.

The findings shown in Figs 3,4 and 5 indicate that the surface modified  $\text{Al}_2\text{O}_3$  exhibits enhanced stability in coolants when compared to pristine  $\text{Al}_2\text{O}_3$ . A significant disparity in the zeta potential is observed between the initial day and the thirtieth day when considering coolants that are dispersed with pristine  $\text{Al}_2\text{O}_3$ .

The suspensions exhibit remarkable stability as evidenced by the little difference in zeta potential over a one-month period, which can be attributed to the dispersion of  $\text{Al}_2\text{O}_3$  surface modified with CTAB. Although SDS could make the suspension stable but the zeta potential is low compared to suspension with CTAB. Cetrimonium bromide operates as a cationic surfactant as a result of its inherent positive charge, and it is employed for the purpose of stabilizing nanoparticles that exhibit a negative surface charge. This can provide significant benefits when dealing with specific types of nanoparticles that demonstrate a negative surface charge, such as various metal oxides. Sodium Dodecyl Sulfate (SDS) is an anionic surfactant frequently employed to stabilize nanoparticles with a positive surface charge. The aforementioned behavior is commonly observed in metallic nanoparticles that possess a positive charge while being dispersed throughout a fluid. The improved stability of the  $\text{Al}_2\text{O}_3$  surface-modified with CTAB in nanofluids can be attributed to the presence of functional groups on its surface. These groups form bonds with the polar groups of ethylene glycol and water molecules, thereby enabling the  $\text{Al}_2\text{O}_3$  nanoparticles to maintain their stability.

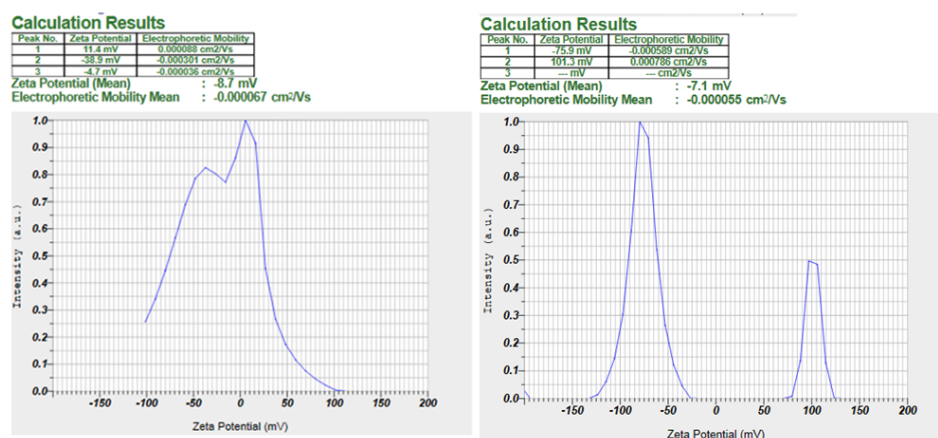


**Figure 3** Zeta potential of Ethylene glycol dispersed with a) pristine 1 %  $\text{Al}_2\text{O}_3$  on first day b) pristine 1 %  $\text{Al}_2\text{O}_3$  after 5 days

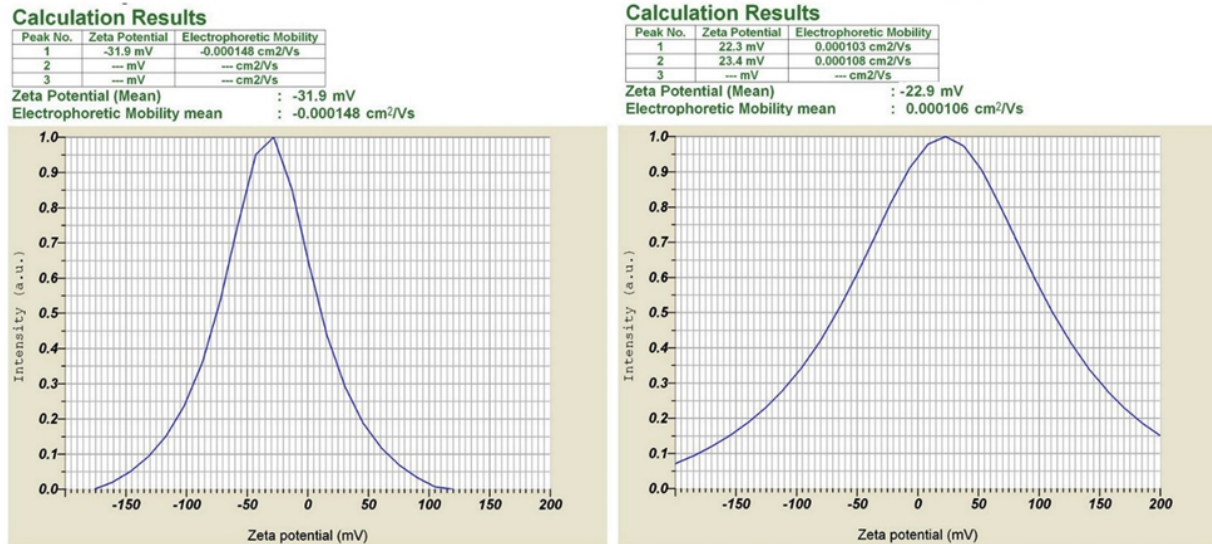


**Figure 4** Zeta potential of Ethylene glycol dispersed with 1 %  $\text{Al}_2\text{O}_3$  surface modified with SDS a) after 15 days  
b) after one month

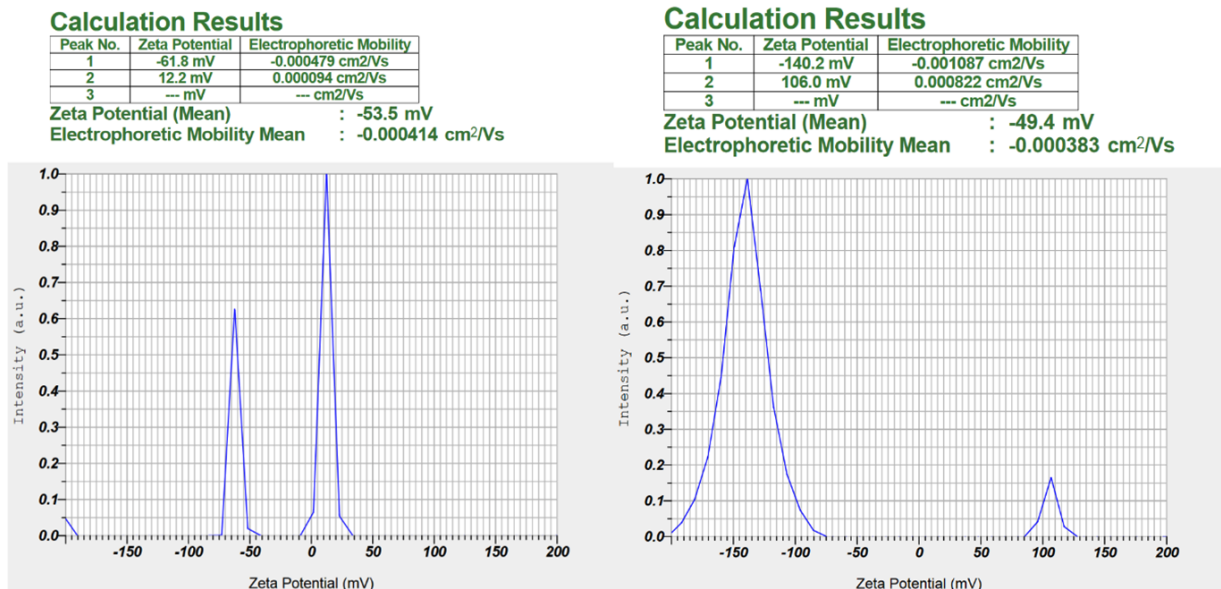


**Figure 5** Zeta potential of Ethylene glycol dispersed with 1 %  $\text{Al}_2\text{O}_3$  surface modified with CTAB a) after 15 days  
b) after one month

**TABLE 2: Zeta potential variation of samples dispersed with  $\text{Al}_2\text{O}_3$  nano particles surface modified with SDS**

Samples dispersed with $\text{Al}_2\text{O}_3$ nanoparticles	Zeta potential, mV with surface modified $\text{Al}_2\text{O}_3$ nano particles	
	1 <sup>st</sup> day	After 2 months
Ethylene glycol+ 0.125% SDS treated $\text{Al}_2\text{O}_3$ nanoparticles	-45.1	-36.7
Ethylene glycol + 0.25% SDS treated $\text{Al}_2\text{O}_3$ nanoparticles	-38.2	-35.1
Ethylene glycol+ 0.5% SDS treated $\text{Al}_2\text{O}_3$ nanoparticles	-36.5	-28.3
Ethylene glycol+1 % SDS treated $\text{Al}_2\text{O}_3$ nanoparticles	-31.1	-22.4



**TABLE 3: Zeta potential variation of samples dispersed with Al<sub>2</sub>O<sub>3</sub> nanoparticles surface modified with CTAB**

Samples dispersed with Al <sub>2</sub> O <sub>3</sub> nanoparticles	Zeta potential, mV with surface modified Al <sub>2</sub> O <sub>3</sub> nano particles	
	1 <sup>st</sup> day	After 2 months
Ethylene glycol+0.125% CTAB treated Al <sub>2</sub> O <sub>3</sub> nano particles	-62.7	-56.8
Ethylene glycol+0.25% CTAB treated Al <sub>2</sub> O <sub>3</sub> nano particles	-58.6	-55.5
Ethylene glycol+ 0.5% CTAB treated Al <sub>2</sub> O <sub>3</sub> nano particles	-57.4	-54.2
Ethylene glycol+1 % CTAB treated Al <sub>2</sub> O <sub>3</sub> nano particles	-53.5	-49.4

**TABLE 3: Zeta potential variation of samples dispersed with pure Al<sub>2</sub>O<sub>3</sub> nano particles**

Samples dispersed with Al <sub>2</sub> O <sub>3</sub> nanoparticles	Zeta potential, mV with pristine Al <sub>2</sub> O <sub>3</sub>	
	1 <sup>st</sup> day	After 5 days
Ethylene glycol+0.125% pure Al <sub>2</sub> O <sub>3</sub> nanoparticles	30.3	10.2
Ethylene glycol+0.25% pure Al <sub>2</sub> O <sub>3</sub> nanoparticles	25.8	8.8
Ethylene glycol+ 0.5% pure Al <sub>2</sub> O <sub>3</sub> nanoparticles	20.8	15
Ethylene glycol + 1 % pure Al <sub>2</sub> O <sub>3</sub> nanoparticles	-8.7	-7.1

### 3.2 Determination of Thermophysical properties of test fluids

The existing literature has consistently demonstrated an enhancement in thermal conductivity with the use of nano materials, as evidenced by numerous research [1-31]. The alumina nanoparticles present in the nanofluid exhibit continuous Brownian motion, which is characterized by stochastic movement. This motion facilitates increased interactions between the nanoparticles and the molecules of the fluid, resulting in a reduction in heat resistance within the fluid. Alumina nanoparticles exhibit a significantly greater surface area in comparison to larger particles or the constituent molecules of the base fluid. The enhanced surface area enables heightened interactions between the nanoparticles and the surrounding fluid, resulting in enhanced heat conductivity.

The dispersion of particles in liquids significantly enhances thermal conductivity, resulting in improved heat transmission. Fig. 6a demonstrate a direct relationship between the proportion of alumina nanoparticles surface modified with CTAB and the corresponding enhancement in thermal conductivity of the nanofluid. The thermal conductivity of nanofluids was observed to be much greater than that of corresponding base fluids across all tested fluids. On the other hand, the heat conductivity of pure ethylene glycol exhibited just a slight rise. The impact of temperature on the improvement of thermal conductivity is also worth noting. The enhancement in thermal conductivity is more pronounced at elevated temperatures. Significant enhancements of 11%, 14%, 18%, and 22% was observed with the utilization of a 0.125, 0.25, 0.5 and 1 % alumina nanoparticles.

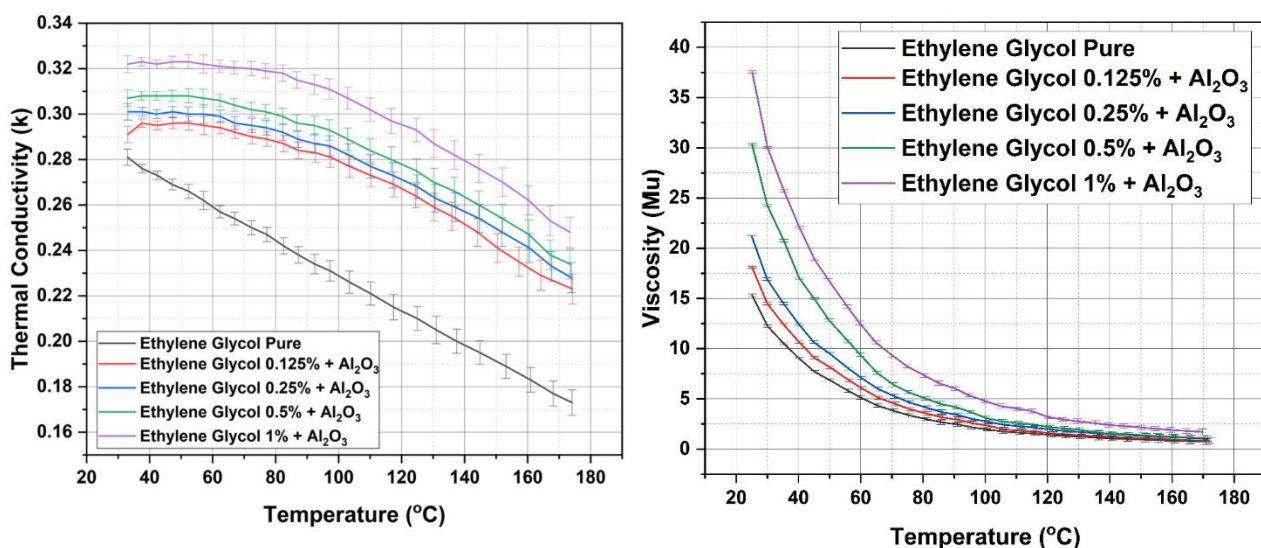


**FIG. 6: Thermal conductivity vs temperature plots for the sample ethylene-glycol with different weight % of Al<sub>2</sub>O<sub>3</sub> nanoparticles surface modified with CTAB**

Figure 6b depicts the temperature-dynamic viscosity graphs of different nanofluids, showing an

increase in Al<sub>2</sub>O<sub>3</sub> weight fractions. Nanofluids demonstrate an observable rise in dynamic viscosity

due to the dispersion of  $\text{Al}_2\text{O}_3$ . This enhancement is solely found within the confines of lower temperature ranges. The increase in dynamic viscosity of nanofluids relative to base liquids is insignificant at elevated temperatures. However, the impact of temperature on the viscosity of nanofluids

containing scattered  $\text{Al}_2\text{O}_3$  is negligible at elevated temperatures, as demonstrated by other prior studies. The specific heat of ethylene glycol–water samples containing  $\text{Al}_2\text{O}_3$  nanoparticles was measured using a C-Therm trident probe. The values are presented in Table 6.

**TABLE 6: The values of specific heat for Ethylene-glycol water mixture with different percentages of  $\text{Al}_2\text{O}_3$  at room temperature**

S. No	Test fluid	Specific heat, $C_p$ , kJ/kg K
1	Ethylene glycol	2.75
2	Ethylene glycol+0.125% $\text{Al}_2\text{O}_3$	2.74
3	Ethylene glycol+0.25% $\text{Al}_2\text{O}_3$	2.73
4	Ethylene glycol+ 0.5% $\text{Al}_2\text{O}_3$	2.72
5	Ethylene glycol+ 1 % $\text{Al}_2\text{O}_3$	3.09

Due to such low concentrations, nanofluids have less specific heat variation compared to their base fluids. As  $\text{Al}_2\text{O}_3$  weight fraction increases, values decline slightly.

### 3.3 Effect of surface modification and choice of surfactant on properties

The thermal conductivity of nanoparticles in nanofluids can be significantly influenced by the surface modification techniques employed. The dispersion of nanoparticles in a nanofluid leads to enhanced thermal contact and improved thermal conductivity. The effect of surface modification with different surfactants and unmodified nanoparticles on thermal conductivity is studied. Fig. 7a compares the thermal conductivity of nanofluids with surface modified and pristine  $\text{Al}_2\text{O}_3$ . It can be seen that the nanofluids unmodified  $\text{Al}_2\text{O}_3$  tend to agglomerate

and lose their properties. The implementation of surface modification techniques has shown effective in mitigating the phenomenon of nanoparticle agglomeration. This, in turn, facilitates a more homogeneous dispersion of nanoparticles within the fluid medium, hence leading to a notable improvement in thermal conductivity. Moreover, enhanced wetting facilitated improved nanoparticle–fluid interaction, resulting in heightened thermal conductivity as a consequence of diminished thermal resistance at the interface between the particles and the fluid. Fig. 7b shows the comparison of the efficacy of SDS and CTAB as surfactants to stabilize  $\text{Al}_2\text{O}_3$ . Both surfactants could improve the thermal conductivity but the improvement is more when nanofluids are prepared with  $\text{Al}_2\text{O}_3$  surface modified with CTAB.

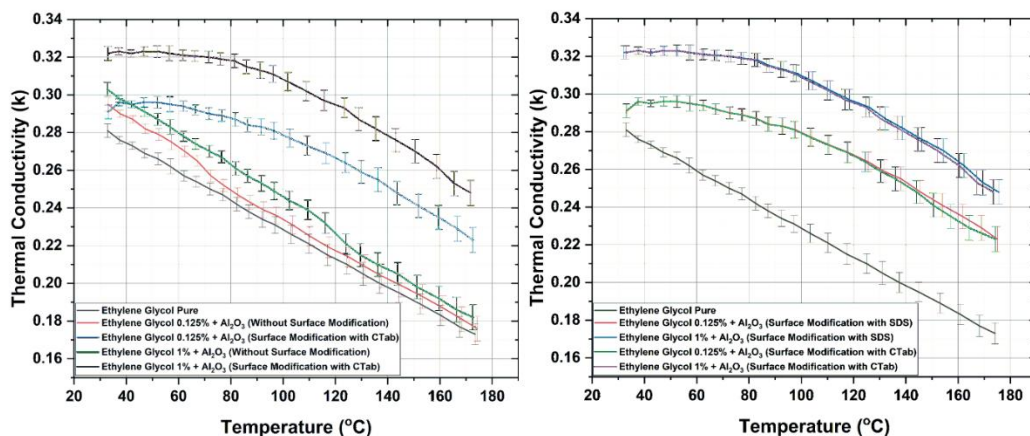


**Fig. 7** Variation of thermal conductivity with temperature a) comparison of thermal conductivity of nanofluids with surface modified and pristine  $\text{Al}_2\text{O}_3$  b) comparison of the efficacy of SDS and CTAB as surfactants

### 3.2 Correlations for thermophysical properties

Various scholars have described the rise in heat conductivity in the prior art. Nevertheless, significant disparities are seen in the experimental findings. Therefore, it is imperative to utilize a mathematical model in order to accurately determine the thermal conductivity and dynamic viscosity of the test fluids. When theoretical values are derived from a predictive model, comparing

them to experimental values enables the assessment of the model's predictive capacity. This aspect holds particular significance when the model is used to generate predictions on novel or unobserved data. In order to evaluate the properties, regression models are constructed by analyzing the experimental data separately for thermal conductivity and dynamic viscosity. The Minitab statistical tool is utilized to develop a nonlinear



mathematical model in this work. The variables being considered include dynamic viscosity and thermal conductivity. The dependent variables in this study are the temperature and the concentration of  $\text{Al}_2\text{O}_3$ . Regression modeling involves multiple iterations before selecting a nonlinear regression model with the lowest prediction error.

At first, the nonlinear model generated a significantly large prediction error. Therefore, all the variables are transformed into logarithmic variables in order to be suitable for a linear model. A nonlinear model was then suggested by transforming the linear model, which is expressed by the following equations.

$$k_{nf} = 1.8(1 + \varphi)^{0.33} \left(1 + \frac{T}{T_{max}}\right)^{0.88} (k_b)^{1.6} \quad (1)$$

$$\mu_{nf} = 12.5(1 + \varphi)^{1.23} \left(1 + \frac{T}{T_{max}}\right)^{-4.3} (\mu_b)^{0.26} \quad (2)$$

The evaluation of the congruence between the theoretical model and the experimental data is facilitated by the analysis of the plot. Figure 8 illustrates the verification of equation 1 and equation 2. The equations predict the dynamic viscosity and thermal conductivity of ethylene glycol nanofluids within a specific range of temperatures and weight percentages of MWCNT. Furthermore, both equations exhibit a maximum deviation of  $\pm 3\%$  from the experimental data.

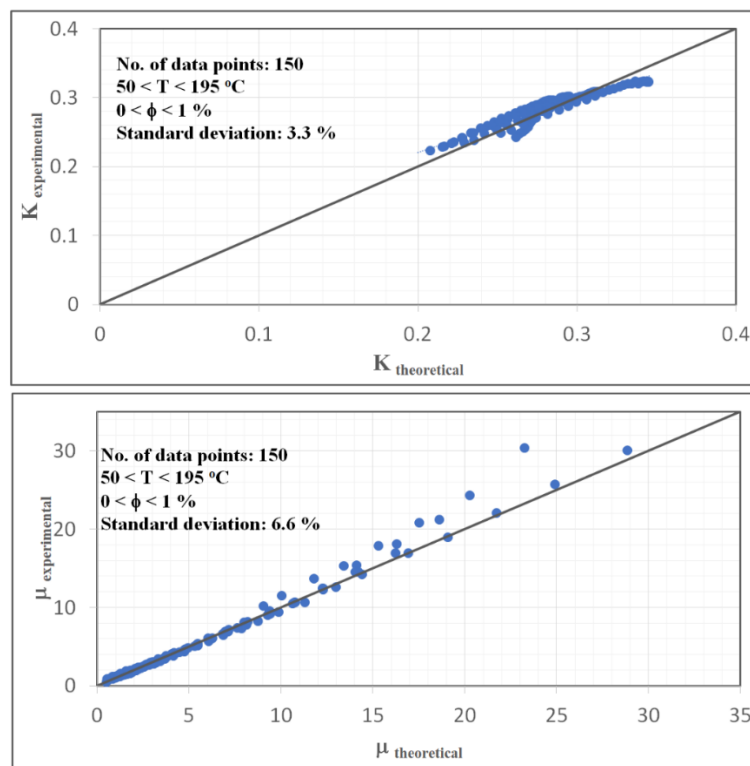


**FIG. 8:** Confirmation of validity of a) Equation 1 for thermal conductivity and b) Equation 2 for Dynamic viscosity

#### 4 CONCLUSIONS

These are the findings based on the results:

1. The zeta potential of nanofluids containing pure  $\text{Al}_2\text{O}_3$  drops rapidly within the first day and one month, indicating poor stability. Nanofluids distributed with surface-modified  $\text{Al}_2\text{O}_3$  have little zeta potential change, indicating remarkable stability.
2. Cetrimonium bromide is considered more suited than sodium dodecyl sulfate for metal oxide nanoparticles.
3. The addition of surface-modified  $\text{Al}_2\text{O}_3$  nanoparticles to the base liquid resulted in an improvement in thermal conductivity by 11-22%.

4. The increase in heat conductivity is highly influenced by the proportion of  $\text{Al}_2\text{O}_3$  nanoparticles and the method used to modify the surface.
5. Within the temperature range of 50 to 70 oC, the viscosity of nanofluids exhibits an upward trend. The increase in thickness at elevated temperatures, however, is insignificant. The impact of surfactant on viscosity is insignificant.
6. A simplified correlation is proposed to predict the effective thermal conductivity and viscosity of ethylene glycol water mixes. This correlation is based on weight fraction and temperature, and is applicable to all possible combinations.

## Acknowledgments

The authors gratefully acknowledge the support received from Hindustan Petroleum Corporation Ltd., Corporate R&D for conducting the tests. The authors acknowledge the assistance from central university, Hyderabad in characterization.

## References

1. Ajeet, K., Dixit, C.K., 3 - Methods for characterization of nanoparticles, Editor(s): Surendra Nimesh, Ramesh Chandra, Nidhi Gupta, Advances in Nanomedicine for the Delivery of Therapeutic Nucleic Acids, Woodhead Publishing, pp 43-58, 2017.
2. E. Dupont, R. Koppelaar, H. Jeanmart, (2020) Global available solar energy under physical and energy return on investment constraints. *Appl. Energy* 257, 113968 (2020)
3. S. Hoseinzadeh, R. Azadi, Simulation and optimization of a solar-assisted heating and cooling system for a house in Northern of Iran. *J. Renew. Sustain. Energy* 9, 045101 (2017)
4. O.O. Bamisile, A.A. Babatunde, M. Dagbasi, I. Wole-Osho, Assessment of solar water heating in Cyprus: utility, development and policy. *Int. J. Renew. Energy Res.* 7, 448–1453 (2017)
5. S. Hoseinzadeh, R. Ghasemiasl, M. A. Javadi, P. S. Heyns, Performance evaluation and economic assessment of a gas power plant with solar and desalination integrated systems. (2020)
6. S. Hoseinzadeh, M. Hadi Zakeri, A. Shirkhani, A.J. Chamkha, Analysis of energy consumption improvements of a zero-energy building in a humid mountainous area. *J. Renew. Sustain. Energy* 11, 015103 (2019)
7. R. Ghasemiasl, S. Hoseinzadeh, M.A. Javadi, Numerical analysis of energy storage systems using two phase-change materials with nanoparticles. *J. Thermophys. Heat Transf.* 32, 440–448 (2018)
8. S.U.S. Choi, J.A. Eastman, Enhancing thermal conductivity of fluids with nanoparticles. *Am. Soc. Mech. Eng. Fluids Eng. Div. FED* 231, 99–105 (1995)
9. H.W. Xian, N.A.C. Sidik, G. Najafi, Recent state of nanofluid in automobile cooling systems. *J. Therm. Anal. Calorim.* 135, 981–1008 (2019)
10. M.U. Sajid, H.M. Ali, Recent advances in application of nanofluids in heat transfer devices : A critical review. *Renew. Sustain. Energy Rev.* 103, 556–592 (2019)
11. Agarwal, R., Verma K., Agrawal, N., Singh, R., Sensitivity of Thermal Conductivity for Al<sub>2</sub>O<sub>3</sub> Nanofluids, *Experimental Thermal and Fluid Science*, vol. 80, pp.19-26, 2017.
12. Das, S. K., Choi, S. U. S., and Patel, H. E., Heat Transfer in Nanofluids – A Review, *Heat Transfer Engineering*, vol.27, no.10, pp.3-19, 2006.
13. Ding, Y., Wen, D., Experimental investigation into convective heat transfer of nanofluid at the entrance region under laminar flow conditions, *Int J Heat Mass Transf.*, vol.47, pp.5181–5188, 2004.
14. Suganthi, K.S., Leela, V.V., Rajan, K.S., Heat transfer performance and transport properties of ZnO–ethylene glycol and ZnO–ethylene glycol–water nanofluid coolants, *Appl. Energy*, vol.135, pp.548–559, 2014.
15. Hemmat, E.M., Saedodin, S., Mahian, O., Wongwises, S., Efficiency of ferromagnetic nanoparticles suspended in ethylene glycol for application in energy devices: effects of particle size, temperature, and concentration, *International Communications in Heat and Mass Transfer*, vol.58, pp.138–146, 2014.
16. Poongavanam, G. K., and Ramalingam, V., Characteristics investigation on thermo physical properties of synthesized activated carbon nanoparticles dispersed in solar glycol, *International Journal of Thermal Sciences*, vol. 136, pp.15–32, 2019.
17. Sridhara, V., Satapathy, L.N. Al<sub>2</sub>O<sub>3</sub>-based nanofluids: a review. *Nanoscale Res Lett* 6, 456 (2011). <https://doi.org/10.1186/1556-276X-6-456>
18. Vadapalli, S., Sagari, J. K., Alapati, H., Kalamalla, V. R., & Su, R. (2023). Heat-transfer enhancement of mono ethylene glycol– water-based solar thermic fluids dispersed with multiwalled carbon nanotubes in a coiled tube heat exchanger. *Journal of Enhanced Heat Transfer*, 30(5).
19. Dosodia, A., Vadapalli, S., Jain, A. K., Mukkamala, S. B., & Sanduru, B. T. (2022). Experimental Studies and Analytical Analysis of Thermophysical Properties of Ethylene Glycol–Water-Based Nanofluids Dispersed with Multi-walled Carbon Nanotubes. *International Journal of Thermophysics*, 43(12), 175
20. Surakasi, R., Sagari, J., Vinjamuri, K. B., Sanduru, B., & Vadapalli, S. (2021). Stability and Thermo-Physical Properties of Ethylene Glycol Based Nanofluids for Solar Thermal Applications. *International Journal of Heat & Technology*, 39(1)
21. He, Q., Zeng, S., Wang, S., Experimental investigation on the efficiency of flat plate solar collectors with nanofluids, *Applied Thermal Engineering Journal*, vol. 88, pp.165-171, 2015.
22. Vaisman, L., Wagner, H. D., and Marom, G., The role of surfactants in dispersion of carbon nanotubes, *Advances in Colloid and Interface Science*, vol. 128–130, pp.37–46, 2006.
23. Vajjha, R. S., Das, D. K., and Chukwu, G. A., An experimental determination of the viscosity of propylene glycol/water based nanofluids and development of new correlations, *Journal of Fluids Engineering, Transactions of the ASME*, vol.137, no.8, 1–15, 2015.

24. Yang, Y., Zhang, Z.G., Grulke, E.A., Anderson, W.B., Heat transfer properties of nanoparticle-in-fluid dispersions (nanofluids) in laminar flow, International Journal of Heat and Mass Transfer, **vol.48**, no.6, pp.1107-1116, 2005.
25. Zhang, X., Gu, H., Fujii, M., Experimental study on the effective thermal conductivity and thermal diffusivity of nanofluids, *Int. J. Thermophys.*, **vol.27**, no.2, pp. 569–580, 2006.